Group II Metabotropic Glutamate Receptor (mGlu2 and mGlu3) Roles in Thalamic Processing

Caroline S Copeland[1,2*], Stuart A Neale[3], Eric S Nisenbaum[4], Thomas E Salt[2,3]

1. Institute of Pharmaceutical Sciences, King's College London, Franklin Wilkins Building, Stamford Street, London, SE1 9NH
2. Institute of Ophthalmology, University College London, 11-43 Bath Street, London, EC1V 9EL
3. Neurexpert Limited, The Core, Bath Lane, Newcastle Upon Tyne NE4 5TF, UK
4. Eli Lilly and Company, 893 S Delaware Street, Indianapolis, IN 46285, USA

*Corresponding author: CSC

CSC: ORCID ID 0000-0002-4462-1402; email caroline.copeland@kcl.ac.uk
SAN: ORCID ID N/A; email stuartneale@neurexpert.com
ESN: ORCID ID 0000-0002-0744-2712; email nisenbaum_eric_s@lilly.com
TES: ORCID ID 0000-0002-6077-6666; email t.salt@ucl.ac.uk

Running title: Group II mGlu receptor roles in thalamic processing

Data availability: Data are available on request from the corresponding author.

Funding: Supported by a Biotechnology and Biological Sciences Research Council (BBSRC) grant (BB/H530570/1 to TES) and Eli Lily & Co.

Author contributions: All authors conceived and planned the experiments. CSC and EN carried out the experiments. All authors contributed to the interpretation of the results. CSC took the lead in writing the manuscript. All authors provided critical feedback and helped shape the research, analysis and manuscript.

Conflict of interest disclosure: The authors have no conflicts of interest to disclose.

Ethics approval: All experimental conditions and procedures were either in accordance with the National Institutes of Health (NIH) regulations of animal care covered in the Principles of Laboratory Animal Care, NIH publication 85-23, revised 1985, and were approved by the Eli Lilly and Company Institutional Animal Care and Use Committee, or were approved by the Home Office (UK) and were in accordance with the UK Animals (Scientific Procedures) Act 1986 and ARRIVE and BJP guidelines.

Word count: 3210 (excluding abstract, methods, references and figure legends).

Abstract

Background and Purpose

As the thalamus underpins almost all aspects of behaviour, it is important to understand how the thalamus operates. Group II metabotropic glutamate (mGlu2/mGlu3) receptor activation reduces inhibition in thalamic nuclei originating from the surrounding thalamic reticular nucleus (TRN). Whilst an mGlu2 component to this effect has been reported, in this study we demonstrate that it is likely largely mediated via mGlu3.

Experimental Approach

The somatosensory ventrobasal thalamus (VB) is an established model for probing fundamental principles of thalamic function. *In vitro* slices conserving VB-TRN circuitry from wild-type and mGlu3 knock-out mouse brains were used to record IPSPs and mIPSCs. *In vivo* extracellular recordings were made from VB neurons in anaesthetised rats. A range of selective pharmacological agents were used to probe Group II mGlu receptor function (agonist: LY354740; antagonist: LY341495; mGlu2 positive allosteric modulator: LY487379; mixed mGlu2 agonist/mGlu3 antagonist: LY395756).

Key Results

The *in vitro* and *in vivo* data are complementary and suggest mGlu3 receptor activation is largely responsible for potentiating responses to somatosensory stimulation by reducing inhibition from the TRN.

Conclusions and Implications

mGlu3 receptor activation in the VB likely enables important somatosensory information to be discerned from background activity. These mGlu3 receptors are likely endogenously activated via 'glutamate spillover'. In cognitive thalamic nuclei, this mechanism may be of importance in governing attentional processes. Positive allosteric modulation of endogenous mGlu3 receptor activation may therefore enhance cognitive function in pathophysiological disease states, such as schizophrenia, thus representing a highly specific therapeutic target.

Key words

Ventrobasal thalamus
Thalamic reticular nucleus
Metabotropic glutamate receptors
Sensory processing
Schizophrenia
Electrophysiology

Abbreviations

CNQX - 6-cyano-7-nitroquinoxaline-2,3-dione
DL-APV - DL-2-Amino-5-phosphonopentanoic acid
DMSO - Dimethyl sulfoxide
i.p. - Intraperitoneal
IPSP – Inhibitory post-synaptic potential
mGlu – metabotropic glutamate receptor
mIPSC – miniature inhibitory post-synaptic current
NIH – National Institutes of Health
TRN – Thalamic reticular nucleus
TTX - Tetrodotoxin
VB – Ventrobasal thalamus

Bullet Point Summaries

What is already known

- The thalamic reticular nucleus provides feedback inhibition to the ventrobasal thalamus upon somatosensory stimulation
- Group II mGlu receptor (mGlu2 and mGlu3) activation reduces this somatosensory evoked inhibition

What this study adds

- mGlu3 receptors likely majority mediate the Group II mGlu effect on sensory evoked inhibition
- These mGlu3 receptors are likely endogenously activated by 'glutamate spillover' upon somatosensory afferent stimulation

Clinical significance

- This mechanism likely enables important sensory information to be discerned from background activity
- In higher-order circuits this mechanism may contribute to cognitive and attentional processes

1.0 Introduction

With over thirty distinct nuclear groups, the thalamus co-ordinates the transfer of information to facilitate many aspects of behaviour, from sensation and movement, to cognition and attention (Sherman and Guillery, 2001). It comprises of highly organised circuits in conjunction with the neocortex to process and filter incoming and outgoing information. The somatosensory thalamic nucleus of rodents, the ventrobasal thalamus (VB), is a central tool in the study of structure-function relationships of these thalamocortical circuits due to the highly-conserved somatotopic representation of each individual facial vibrissae as a single barreloid (see Review: (Diamond et al., 2008)). Identifying the structure and function of somatosensory VB microcircuits enables identification of basic principles of thalamic function, which is essential for understanding how the rest of the thalamus operates.

The VB receives excitatory inputs exclusively from the principal sensory trigeminal nucleus via the lemniscal pathway (see Review: (Diamond et al., 2008)). Common to all thalamic nuclei, VB thalamocortical afferents project to layer IV of the cortex, and also receive reciprocal modulatory corticothalamic inputs from layer VI, which modulate how driver inputs are transmitted (see Review: (Jones, 2009)). Both thalamocortical and corticothalamic afferents also innervate the associated thalamic reticular nucleus (TRN), which serves to provide both feedback and feedforward inhibition to thalamic nuclei upon thalamocortical and corticothalamic innervation, respectively (Jones, 2009) (**FIGURE 1**). It is important to understand how this inhibition is controlled, as its maladaptation has been implicated in several neurophysiological disease states, including schizophrenia (Ferrarelli and Tononi, 2017, Steullet et al., 2018, Young and Wimmer, 2017).

It has been extensively documented that Group II metabotropic glutamate (mGlu) receptors within this circuitry play a pivotal role in controlling this inhibition from the TRN to the VB. Electrophysiological studies have shown that activation of Group II mGlu receptors disinhibits sensory-evoked responses in the VB (Salt and Eaton, 1995a, Salt and Eaton, 1995b, Salt and Turner, 1998, Copeland et al., 2012, Turner and Salt, 2003, Cox and Sherman, 1999, Copeland et al., 2017), with ultrastructural studies indicating the presence of Group II mGlu receptors on TRN terminals and surrounding glial processes (Liu et al., 1998, Mineff and Valtschanoff, 1999, Tamaru et al., 2001).

The similarity in sequence homology and subsequent pharmacology of the mGlu2 and mGlu3 receptors (Conn and Pin, 1997) has made it difficult to discern the relative contributions of each subtype to the overall Group II mGlu receptor effect on inhibition from the TRN to the VB. However, with careful use and application of specific pharmacological compounds in a series of electrophysiological experiments, we have previously been able to demonstrate mGlu2 receptor-mediated disinhibition of sensory-evoked responses in the VB (Copeland et al., 2017, Copeland et al., 2012), and as presented in this study we are now able to demonstrate contribution of mGlu3 receptors to this same effect.

2.0 Methods

2.1 Ethical approval

All experimental conditions and procedures were either in accordance with the National Institutes of Health (NIH) regulations of animal care covered in the Principles of Laboratory Animal Care, NIH publication 85-23, revised 1985, and were approved by the Eli Lilly and Company Institutional Animal Care and Use Committee, or were approved by the Home Office (UK) and were in accordance with the UK Animals (Scientific Procedures) Act 1986 and ARRIVE and BJP guidelines (McGrath et al., 2015, Curtis et al., 2015).

2.2 *In vitro* electrophysiology

2.21 Animals

Male mGlu3 knock-out (18-23 days old; n=6; from Jackson Laboratories, USA, on a C57BL6/J background) and wildtype C57BL6/J mice (18-23 days old; n=6; Harlan, USA) were deeply anaesthetised with 4.0% isoflurane and decapitated into a container of crushed ice. Wildtypes (-/-) were bred from heterozygous (+/-) bred pairs. Power calculations were performed to determine animal numbers required based on an estimated signal-to-noise ratio of 2 [mean:standard deviation].

2.22 Slice preparation and recording

Mouse brains were quickly removed and placed in an oxygenated, ice cold beaker of slicing solution which contained (in mM): 110 NaCl; 10 $MgCl_2$; 2 KCl; 26 $NaHCO_3$; 1.25 NaH_2PO_4; 0.5 $CaCl_2$; 10 HEPES and 15 glucose (pH adjusted to 7.45 with NaOH, osmolarity was 308 to 312 mOsm). After cooling in slicing solution for 2 to 3 minutes, the whole brains were blocked (portions of anterior and posterior tissue removed) using a razor blade and then glued to the microslicer (DTK Zero 1, DSK) tray using cyanoacrylate. The tray containing the blocked and mounted brain was filled with oxygenated, ice cold slicing solution and serial, coronal sections containing the TRN and VB were cut at a thickness of 300-400µm. Slices were then placed in a larger recovery chamber containing oxygenated slicing solution at room temperature (18 to 20°C). The recovery chamber was in a large water bath at room temperature. Slices for inhibitory post-synaptic potential (IPSP) and mini-inhibitory post-synaptic current (mIPSC) recordings were processed as follows.

2.221 IPSP recordings

After 1h in the recovery chamber, medium was replaced by a continuously oxygenated Krebs medium containing (in mM): 124 NaCl, 3 KCL, 1.25 KH_2PO_4, 1 $MgSO_4$, 2 $CaCl_2$, 26 $NaHCO_3$ and 10 glucose. After a further hour, slices were then transferred to an interface recording chamber mounted on a Nikon Eclipse FN-1 microscope where they were perfused with the same continuously oxygenated Krebs medium. Using the current clamp technique, intracellular recordings were made from neurons in the VB with sharp standard-walled glass microelectrodes, filled with 1M potassium acetate (final tip resistance: 80-120MOhm). To generate synaptic events of cortical and/or TRN origin, a bipolar stimulating electrode was placed on the border of the VB and TRN. The slice was then superfused with recording solution containing 10µM 6-cyano-7-nitroquinoxaline-2,3-dione (CNQX), 50µM DL-2-Amino-5-phosphonopentanoic acid (DL-APV) and 0.5µM tetrodotoxin (TTX) to block the AMPA- and NMDA- evoked miniature and large amplitude events due to direct action potential firing of inhibitory neurons, respectively, leaving only the GABA mediated synaptic events (confirmed in preliminary experiments by complete blockade of remaining synaptic events with 10µM bicuculline).

Stimulation of the TRN at low frequency (0.1Hz) using 100µs square wave pulses of current (30-500µA) evoked an IPSP. Input resistance was determined by measuring the voltage drop due to passing a -0.05 or -0.1nA current pulse through the electrode. After several baseline response cycles displaying

consistent neuronal responses had been recorded, compound-containing solutions were applied unblinded to the slice via whole chamber superfusion. After cessation of compound application, recordings were continued until neuronal responses had returned to their respective baseline response levels. (1S,2S,5R,6S)-2-Aminobicyclo[3.1.0]hexane-2,6-dicarboxylic acid (LY354740) and (2S)-2-Amino-2-[(1S,2S)-2-carboxycycloprop-1-yl]-3-(xanth-9-yl) propanoic acid (LY341495) stocks were made in 100% dimethyl sulfoxide (DMSO) at 1000X the desired working concentration. Compound was diluted into the recording solution containing CNQX, APV and TTX immediately before application to the brain slice. All solutions applied to the brain slices contained 0.1% to 0.2% DMSO. DMSO content was matched between solutions for each experimental protocol and in the vehicle controls. Compound treatment periods were from 10 to 12 minutes in duration.

2.222 mIPSC recordings

After a 10 minute period in the recovery chamber, 500µL of 0.5M $CaCl_2$ solution was slowly added (500ml volume) to increase the calcium concentration to 1mM. The water bath was then turned on and the temperature was monitored inside the recovery chamber. The recovery chamber temperature was allowed to reach 33 to 34°C for a period of approximately 30 minutes, after which the water bath was turned off and the recovery chamber was allowed to slowly return to room temperature (18 to 20°C). Slices were used for recording after at least 1 hour of recovery time.

Slices were placed in a superfusion chamber mounted on a Nikon Eclipse FN-1 microscope. Neurons within the VB area of the thalamus were visualized using IR/DIC water immersion optics. The recording solution was composed of (in mM): 115 NaCl; 1.5 $MgCl_2$; 5 KCl; 26 $NaHCO_3$; 1.25 NaH_2PO_4; 10 HEPES; 2 $CaCl_2$ and 15 glucose at pH 7.45, oxygenated with carbogen gas (95%O_2/5%CO_2) and osmolarity of 300 to 305 mOsm. The brain slice in the chamber was continually superfused at a rate of 3mL/min with oxygenated recording solution (18 to 20°C) containing 10µM CNQX, DL-APV and 0.5µM TTX to block the AMPA- and NMDA- evoked miniature and large amplitude events due to direct action potential firing of inhibitory neurons, respectively, leaving only the GABA mediated synaptic events. Compound containing solutions were applied to the slice via whole chamber superfusion. Glass recording electrodes were filled with (in mM): 140 CsCl; 1 $MgCl_2$; 10 HEPES; 3 NaATP; 0.3 NaGTP; 1 Cs-EGTA at pH 7.2 and osmolarity adjusted to 294 to 300 mOsm and had a resistance of 2 – 4MΩ.

Visualized neurons were patch clamped in whole cell configuration (Multiclamp 700B, MDS) and access resistance (Ra) was evaluated in voltage clamp mode. A gapfree protocol (Clampex V10, MDS) with a holding potential of -70mV was used to record miniature synaptic events until the access resistance and holding current were stable in recording solution only. LY354740 and LY341495 stocks were made in 100% DMSO at 1000X the desired working concentration. Compounds were diluted into the recording solution containing CNQX, APV and TTX immediately before application to the brain slice. All solutions applied to the brain slices contained 0.1% to 0.2% DMSO. DMSO content was matched between solutions for each experimental protocol and in the vehicle controls. After several baseline response cycles displaying consistent neuronal responses had been recorded, compounds were applied unblinded in time periods ranging from 10 to 12 minutes in duration as required. After cessation of compound application, recordings were continued until neuronal responses had returned to their respective baseline response levels.

2.3 *In vivo* single neuron recording and iontophoresis

2.31 Animals

All experiments were conducted using adult male Wistar rats (380-450g, n=14, Harlan, UK) housed on a 12h light/dark cycle with food and water ad libitum. There are no evident gender differences in rat acute electrophysiological responses (Becker et al., 2016). Power calculations were performed to

determine animal numbers required for each experimental protocol based on an estimated signal-to-noise ratio of 2 [mean:standard deviation].

2.32 Surgery

Animals were anaesthetised with urethane (1.2g/kg intraperitoneal [i.p.] injection) and were prepared for recording as previously described (Salt, 1987). Throughout the experiments, electroencephalogram and electrocardiogram were monitored. Additional urethane anaesthetic was administered i.p. as required, and the experiment was terminated with an overdose of the same anaesthetic.

2.33 Recording and iontophoresis

Seven-barrel recording and iontophoretic glass pipettes were advanced into the VB. Extracellular recordings were made from single VB neurons responsive to somatosensory input through the central barrel (filled with 4M sodium chloride [NaCl]). Iontophoretic drug applications were performed unblinded using the outer barrels (Salt, 1987). On each occasion, one of the outer barrels was filled with 1M NaCl for current balancing. The remaining outer barrels each contained one of the following substances: LY354740, LY341495, (1S,2S,4R,5R,6S)-rel-2-Amino-4-methylbicyclo[3.1.0]hexane-2,6-dicarboxylic acid (LY395756) as Na^+ salts (each 5mM, pH8.0 in 75mM NaCl), ejected as anions, with 2,2,2-Trifluoro-N-[4-(2-methoxyphenoxy)phenyl]-N-(3-pyridinylmethyl)ethanesulfonamide hydrochloride (LY487379; 1mM, pH6.0, in 1% DMSO, 75mM NaCl) ejected as cations, and a 1% DMSO vehicle control. All compounds were prevented from diffusing out of the pipette by using a retaining current (10-20nA) of opposite polarity to that of the ejection current. Compounds were ejected within a current range ensured to produce a sub-maximal effect on sensory inhibition (LY354740 6nA-50nA; LY341495 12-40nA; LY395756 10-50nA; LY487379 50nA-100nA).

2.34 Stimulation protocol

Neurons were identified as VB neurons on the basis of stereotaxic location (Paxinos and Watson, 1986) and responses to vibrissa deflection. Vibrissa deflection was performed using fine air-jets directed through 23 gauge needles mounted on micro-manipulators positioned and orientated close to the vibrissa to ensure deflection of a single vibrissa was achieved. Air-jets were electronically gated with solenoid valves that produced a rising air pulse at the vibrissa 8ms after switching. Response latencies were calculated from the start of the gating pulse. Using such an approach it is possible to use air-jets to evoke an excitatory response from stimulation of a single vibrissa, as described previously (Salt, 1987). Prior to the beginning of the experimental protocol, the 'principal' vibrissa (i.e. the vibrissa at the centre of the receptive field) for each neuron was identified. All neurons recorded from were quiescent.

Cycles of sensory stimulation (10s long) were established and repeated continuously whilst recording from neurons. Cycles contained one type of stimulus consisting of 500-1000ms duration trains (5-10Hz) of air-jets directed at the principal vibrissa. After several baseline response cycles displaying consistent neuronal responses had been recorded, LY354740, LY341495, LY487379 and/or LY395756 were iontophoretically ejected for 2-15mins as required. After cessation of compound ejection, sensory stimulation cycles were continued until VB neuronal responses had returned to their respective baseline response levels.

2.4 Data collection and statistical analysis

In vitro electrophysiology protocols: mIPSC signals were amplified, low-pass filtered at 5kHz, digitised with an analog-to-digital converter and collected onto a computer hard drive and analysed with the MiniAnalysis program (V6.0.4, Synaptosoft). Quantitative results are expressed in the text and figures as mean±S.E.M. MATLAB (Mathworks, Version R2018a) was used to perform paired t-tests to assess

statistical significance (p<0.05). The frequency of the mIPSC events was determined during the final 5 minutes of each treatment period (baseline, 30nM LY354740, 30nM LY354740 + 100nM LY341495) using the MiniAnalysis program (V6.0.4, Synaptosoft). Inter-event intervals were calculated and plotted as cumulative fraction histograms for each treatment group. MATLAB (Mathworks, Version R2018a) was used to perform Kolmogorov-Smirnov tests on the inter-event interval cumulative fractions and Wilcoxon matched pairs tests on mIPSC frequencies to determine statistical significance (p<0.05).

In vivo electrophysiology protocols: Throughout the study, extracellular single neuron action potentials were gated, timed and counted using a window discriminator, a CED1401 interface and Spike2 software (Cambridge Electronic Design, Cambridge, UK), which recorded the output from the iontophoresis unit and also triggered the sensory stimuli sequence. Data were analysed by plotting post-stimulus time histograms (PSTHs) from these recordings by counting the spikes evoked by sensory stimulation. We used conventional criteria to divide neuronal responses into burst and tonic activity (Lu et al., 1992). Any action potentials with interspike intervals of ≤4ms were considered to be part of a burst. All other spikes were regarded as tonic. We computed a burst-tonic firing ratio (the proportion of burst spikes normalized with respect to the total number of recorded spikes). Data are expressed as a percentage of baseline responses prior to compound application to mitigate variability in neuronal responses between cells and aid in interpretation (±S.E.M.). Statistical analysis was performed using MATLAB (Mathworks, Version R2018a), with comparisons made using Wilcoxon matched-pairs test (p<0.05).

2.5 Materials

In vitro electrophysiology protocols: Slice preparation and recording solution components (NaCl, $MgCl_2$, KCl, $NaHCO_3$, NaH_2PO_4, $CaCl_2$, HEPES, KH_2PO_4, $MgSO_4$, glucose, NaOH, CH_3COOK, CsCl, NaATP, NaGTP, Cs-EGTA) and DMSO were obtained from Sigma-Aldrich. CNQX and DL-APV were obtained from Tocris, with TTX and bicuculline obtained from Abcam. LY354740 and LY341495 stocks were made in-house.

In vivo electrophysiology protocols: NaCl and DMSO were obtained from Sigma Aldrich. LY354740, LY341495 and LY487379 were obtained from Tocris. LY395756 was obtained from Dr James Monn, Eli Lilly & Co.

2.6 Nomenclature of Targets and Ligands

Key protein targets and ligands in this article are hyperlinked to corresponding entries in http://www.guidetopharmacology.org, the common portal for data from the IUPHAR/BPS Guide to PHARMACOLOGY (Harding et al., 2018), and are permanently archived in the Concise Guide to PHARMACOLOGY 2019/20 (Alexander et al., 2019).

3.0 Results

The interpretation of the results in this study clearly rely upon careful and appropriate use of the electrophysiological preparations in conjunction with the Group II mGlu receptor selective pharmacological compounds.

The rodent VB comprises one major cell type, thalamocortical relay neurons, and is otherwise largely devoid of intrinsic inhibitory interneurons, receiving its inhibitory input almost exclusively from the adjacent TRN (Diamond et al., 2008). This VB circuitry is homologous between rat and mouse species (Diamond et al., 2008). In this study *in vitro* electrophysiology was performed with mouse brain slices to take advantage of the genetic manipulations possible in this species to generate mGlu3 knock-out animals (Linden et al., 2005). Rats were used for the *in vivo* components to take advantage of their larger vibrissal pad size (Haidarliu et al., 2010), which increases feasibility of individual vibrissa deflections.

The Group II orthosteric agonist LY354740 (Monn et al., 1997, Schoepp et al., 2003) has been widely employed to investigate Group II mGlu receptor function in both *in vitro* and *in vivo* neurophysiological assays in both animal and human CNS studies (Moldrich et al., 2003, Schoepp et al., 2003, Nordquist et al., 2008, Copeland et al., 2012, Copeland et al., 2015, Copeland et al., 2017). The Group II orthosteric antagonist LY341495 possesses high selectivity with nanomolar potencies for the Group II mGlu receptors. Whilst LY341495 also has submicromolar potencies at other mGlu receptor subtypes (Kingston et al., 1998), its use in this study follows the parameters previously demonstrated to produce selective antagonism for the Group II mGlu receptors only (Kingston et al., 1998). The mGlu2 selective PAM LY487379, which possesses no intrinsic agonist activity at mGlu2 receptors, acts to enhance responses to submaximal mGlu2 receptor agonism without activity at other receptors or ion channels (Johnson et al., 2003). The use of LY487379 in rodent *in vitro* and *in vivo* neurophysiological studies is well documented (Galici et al., 2005, Copeland et al., 2012, Copeland et al., 2015, Copeland et al., 2017, Mango et al., 2019, Cieślik et al., 2020). LY395756 is a mixed compound in that it possesses opposite activity at each of the Group II mGlu receptor sub-types: it is an agonist at mGlu2 receptors (EC_{50} 0.40μM) and an antagonist of mGlu3 receptors (IC_{50} 2.94μM; see compound 13 (Dominguez et al., 2005)). Whilst the mGlu2 partial agonist activity of LY395756 has been debated to account for some of its observed pharmacological responses (Johnson et al., 2017, Sanger et al., 2013), under physiological conditions in native systems relevant to the experimental preparations used here, the majority of studies where LY395756 (and/or LY541850, its active enantiomer) has been used demonstrate it to act as a full agonist at mGlu2 receptors: acute (depression) effects are comparable to that of other widely used Group II mGlu receptor agonists (Ceolin et al., 2011, Hanna et al., 2013, Lucas et al., 2013).

3.1 Synaptic transmission at the TRN-VB synapse can be modulated by mGlu3 receptor activation

It has been previously demonstrated that IPSPs evoked *in vitro* in the VB upon TRN stimulation in rat brain slices can be suppressed by Group II mGlu receptor activation (Turner and Salt, 2003), and that there is an mGlu2 component to this overall Group II mGlu effect (Copeland et al., 2012, Copeland et al., 2017). Therefore, we wanted to determine if there was a complementary mGlu3 component to this same effect. Whilst the reversible Group II agonist LY354740 effect on evoked IPSP amplitude in the VB was reproducible in wild-type mouse brain slices (Turner and Salt, 2003, Copeland et al., 2017) where the circuitry connecting the VB and TRN is preserved (LY354740 30nM reduced baseline evoked IPSP amplitude by 29±2%; n=6 cell recordings from 6 slices; **Figures 2ai and 2bi**), this was completely ablated in the mGlu3 receptor knock-out mouse brain slices (LY354740 30nM and 300nM reduced baseline evoked IPSP amplitude by 2±1% and 1±1%, respectively; n=6 cell recordings from 6 slices; **Figures 2aii and 2bii**). Interestingly, upon application of the highest concentration of the Group II

antagonist LY341495 in combination with the Group II agonist LY354740 in the wild-type preparation, an increase in evoked IPSP amplitude when compared to baseline was observed (LY354740 30nM and LY341495 100nM increased evoked IPSP amplitude by 13±2%; **Figures 2ai and 2bi**). Application of vehicle controls had no effect in comparison to baseline responses (data not shown).

One component that contributes to IPSP amplitude suppression is direct inhibition of GABAergic vesicle fusion with the presynaptic TRN membrane (Turner and Salt, 2003). *In vitro* recording of mIPSCs from VB neurons enables quantification of the frequency of such spontaneous presynaptic quantal release events. Whilst the Group II agonist LY354740 effect on mIPSC frequency was reproducible (Copeland et al., 2017) and reversible in wild-type mouse brain slices (**Figure 2ci and 2di**), again, this was not evident in the mGlu3 receptor knock-out mouse brain slice preparations (**Figure 2cii and 2dii**). The frequency of mIPSCs between wild-type and mGlu3 knock-out preparations were comparable (4.1±1.9Hz vs 3.8±1.8Hz, respectively; each n=6 cell recordings from 6 slices; Wilcoxon matched pairs test $p>0.05$). Application of vehicle controls had no effect in comparison to baseline responses (data not shown).

Taken together these *in vitro* data indicate that there is a considerable mGlu3 receptor-mediated component to the overall Group II mGlu receptor effect on TRN-induced GABAergic inhibition evoked in the VB. We therefore sought to confirm this effect *in vivo*.

3.2 mGlu3 activation contributes to the gating of neuronal responses to somatosensory stimulation

VB neuronal responses to short- and long-duration vibrissal stimulation can be potentiated by Group II mGlu receptor activation leading to somatosensory disinhibition, which comprises an mGlu2 component (Salt and Eaton, 1995a, Salt and Eaton, 1995b, Salt and Turner, 1998, Copeland et al., 2012, Copeland et al., 2017). We used iontophoretic application of the mixed compound LY395756 (mGlu2 agonist, mGlu3 antagonist) onto VB neurons *in vivo* to confirm functional contribution of an mGlu3 component to this overall Group II effect, as suggested by the *in vitro* experiments. Application of the mixed compound LY395756 alone inhibited total VB neuronal responses to long duration vibrissal stimulation (83±3% of baseline; n=11 cell recordings from 9 rats; **Figure 3**): an effect similar to that observed upon application of the Group II mGlu antagonist LY341495 (81±5% of baseline; n=6 cell recordings from 3 rats **Figure 4b**). As the mixed compound is an mGlu3 antagonist, this has revealed an mGlu3 component to the overall Group II mGlu effect on sensory disinhibition. Upon co-application of the mixed compound LY395756 with the mGlu2 PAM LY487379 the reverse was seen, with a potentiation of VB neuronal responses to long duration vibrissal stimulation (146±10% of baseline; n=6 cell recordings from 5 rats): an effect similar to that observed upon application of the Group II mGlu agonist LY354740 (177±24% of baseline; n=6 cell recordings from 6 rats; **Figure 4b**). As the mixed compound is an mGlu2 agonist, this confirms the mGlu2 component to the overall Group II mGlu effect on sensory disinhibition that has been previously described (Copeland et al., 2012, Copeland et al., 2017). Furthermore, this action of the mGlu2 PAM confirms that the Harlan Wistar rats used in this study express functional mGlu2 receptors (Ceolin et al., 2011). Application of vehicle controls had no effect in comparison to baseline responses (data not shown).

To further investigate the agonist/antagonist activity of the mixed compound LY395756 we performed further sub-analysis of its effects on burst firing of VB thalamic neurons, which exhibit two distinct response patterns: tonic and burst-mode responses (Ramcharan et al., 2000, Rivadulla et al., 2003, Copeland et al., 2015). Tonic responses are associated with a linear transmission of information, and occur when thalamic neurones have been depolarised from resting potential following the inactivation of a voltage- and time-dependent calcium current (I_T), whilst burst-mode firing occurs following hyperpolarisation of thalamic neurones where I_T is de-inactivated (Llinás and Jahnsen, 1982, Jahnsen and Llinás, 1984). As such, during tonic firing synaptic transmission through the thalamus is faithfully

relayed, whereas during burst firing transmission through the thalamus is less reliable with impulses occurring at low and irregular rates punctuated by high-frequency bursts. Iontophoretic application of the mixed compound LY395756 alone increased burst firing (baseline burst firing: 65±7%; +LY395756 burst firing 75±6%; n=11 cell recordings from 9 rats; **Figure 4a**), an effect similar to that observed upon application of the Group II mGlu antagonist LY341495 (baseline burst firing: 49±6%; +LY341495 burst firing 65±4%; n=6 cell recordings from 3 rats; **Figure 4b**). Iontophoretic application of the mixed compound LY395756 in combination with the mGlu2 PAM LY487379 decreased burst firing (baseline burst firing: 66±6%; +LY395756 & LY487379 burst firing 53±6%; n=6 cell recordings from 5 rats; **Figure 5a**), an effect similar to that observed upon application of the Group II mGlu agonist LY354740 (baseline burst firing: 74±5%; +LY354740 burst firing 62±4%; n=6 cell recordings from 6 rats; **Figure 5b**). Application of vehicle controls had no effect in comparison to baseline responses (data not shown).

4.0 Discussion and Conclusions

Thalamic nuclei can be classed as either first-order or higher-order nuclei based upon the source of their driver inputs of information: first-order nuclei receive driver inputs from the periphery (e.g. auditory, visual, somatosensory), while higher-order nuclei receive driver inputs from cortical layer V (Jones, 2009). By understanding basic principles of thalamic function in a first-order nucleus, such as the VB, it is then possible to extend this basic knowledge to understand the function of more complex thalamic circuitries, such as those of the higher-order thalamic nuclei that serve to support cognitive processes (see Jones [2009] for review). As the rodent VB comprises only of excitatory VB neurons (i.e. no interneurons) (Ralston, 1983, Barbaresi et al., 1986, Harris and Hendrickson, 1987, Ohara and Lieberman, 1993), which when coupled with our in-depth understanding of its simple circuitry (Sherman and Guillery, 2001) (**Figure 1**), makes it an ideal candidate with which to understand the basic principles of thalamic function.

There is substantial evidence from *in vitro* and *in vivo* electrophysiological studies that upon driver afferent stimulation, the Group II mGlu receptors reduce inhibition in thalamic nuclei, likely via a reduction in GABAergic transmission from the TRN (Turner and Salt, 2003, Salt and Eaton, 1995a, Salt and Turner, 1998, Alexander and Godwin, 2005, Copeland et al., 2012, Copeland et al., 2015, Copeland et al., 2017). In the VB it has been previously demonstrated that this mechanism comprises an mGlu2 component (Copeland et al., 2012, Copeland et al., 2017), and in this study we are able to provide further evidence to support this, and also additional evidence for co-contribution from mGlu3 receptor activation to this effect. In fact, these data suggest that the overall Group II mGlu receptor effect is majority mediated via mGlu3: the mixed compound LY395756 is a more than seven-fold more potent mGlu2 receptor agonist (EC_{50} 0.40μM) than it is an mGlu3 receptor antagonist (IC_{50} 2.94μM; (Dominguez et al., 2005)), yet the over-riding effect of the mixed compound when applied alone in this study was that of antagonism. Indeed, the mGlu2 PAM used to reveal the mGlu2 component is in itself very effective: application of submaximal glutamate (1μM) to produce a ~3% of maximal glutamate response can be potentiated upon co-application of LY487479 up to ~75% of maximal glutamate response – a 2500% increase (Johnson et al., 2003) - meaning that even low levels of mGlu2 activation can be revealed. Therefore, the mGlu2 effect revealed by the potent mGlu2 PAM in this study and our previous work (Copeland et al., 2012; Copeland et al., 2017) on reducing inhibition in the VB from the TRN may, under normal physiological conditions, minimally contribute to the overall Group II mGlu effect. Evidence from ultrastructural studies support this theory, as mGlu3 receptors are heavily localised within GABAergic terminals of the TRN (Ohishi et al., 1993a, Ohishi et al., 1993b, Lourenço Neto et al., 2000, Tamaru et al., 2001). Taken together, the electrophysiological and ultrastructural studies suggest that mGlu3 receptors localised on TRN axon terminals likely majority mediate the reduction in inhibition in thalamic nuclei from the TRN, with any Group II mGlu receptor subtypes present on surrounding glial processes likely contributing a smaller modulatory role to the same effect.

The location of Group II mGlu receptors on TRN terminals and surrounding astrocytic processes indicates they play a pivotal role in modulating inhibition in the thalamus. As TRN terminals are not directly targeted by synaptically released glutamate, these receptors may be activated by endogenous 'glutamate spillover' (Kullmann, 2000) from synapses formed between excitatory driver afferents and thalamocortical neurons upon normal sensory processing (Copeland et al., 2012) or under conditions of intense synaptic activation (Alexander and Godwin, 2006). This is further evidenced by the *in vitro* IPSP experiments conducted in this study, as application of the highest concentration of the Group II mGlu receptor antagonist LY341495 was able to increase IPSP amplitude above that seen under baseline conditions. As the mGlu3 knock-out data indicates that reductions in IPSP amplitude and

mIPSC frequency are majority mediated via mGlu3, taken together these data suggest that it is basal mGlu3 receptor activation which is likely occurring upon driver afferent stimulation via 'glutamate spillover' to reduce inhibition in the VB from the TRN. Ultrastructural studies support such a mechanism as they have evidenced close association of sensory afferent terminals with TRN afferent GABAergic terminals, upon which mGlu3 receptors are heavily localized (Ohishi et al., 1993a, Ohishi et al., 1993b, Lourenço Neto et al., 2000, Tamaru et al., 2001), on the soma and proximal dendrites of neurons in the rodent VB (Ralston, 1983, Ohara and Lieberman, 1993).

This study contributes to the growing evidence demonstrating that GABAergic transmission from the TRN can be reduced through activation of Group II mGlu receptors, resulting in a reduction in sensory-evoked inhibition (Copeland et al., 2012, Copeland et al., 2017). Such a mechanism could play an important role in discerning relevant information from background activity to enhance sensory perception. In higher-order nuclei this mechanism could be of importance in attentional and cognitive processes, and there is evidence to suggest that it is the mGlu3 receptor subtype which plays a role in reducing inhibition from the TRN in such nuclei (Copeland et al., 2015).

As increased inhibition in the higher-order mediodorsal thalamic nucleus has been associated with onset of cognitive deficits and impairments in working memory, such as is seen in schizophrenia (Parnaudeau et al., 2013, Peräkylä et al., 2017, DeNicola et al., 2020), targeting of the Group II mGlu receptors, and specifically the mGlu3 receptor subtype, may be of therapeutic importance for this disease state: as antagonism of mGlu3 receptors increases evoked inhibition from the TRN, as evidenced in this study by a decrease in total firing but an increase in burst firing upon application of the mixed compound LY395756 alone, activation of mGlu3 receptors to reduce inhibition may be an appropriate target-specific treatment for schizophrenia. This mechanism of mGlu3-mediated reduction in inhibition is further supported by the IPSP and mIPSC data presented in this study. It has been previously demonstrated that activation of mGlu3 receptors in the mediodorsal thalamus is able to reduce inhibition from the TRN (Copeland et al., 2015), and this study suggests that mGlu3 receptor activation will decrease the unreliable and irregular synaptic transmission associated with burst firing, and increase the proportion of tonic firing where synaptic transmission through the thalamus is faithfully relayed. Indeed, the mGlu3 receptor has been implicated in the aetiological, pathophysiological and pharmaco-therapeutic aspects of schizophrenia, with polymorphisms in the mGlu3 receptor gene and protein, but not the mGlu2 receptor, detected in patients with schizophrenia (See Review: (Stansley and Conn, 2018)). The design of future novel therapies targeted to treat deficits in cognitive function may therefore achieve greater success if selectivity and higher efficacy for mGlu3 receptors were achieved.

4.1 Conclusions

The Group II mGlu receptor effect in reducing evoked inhibition from the TRN to the VB is likely majority mediated via mGlu3 receptors. This mechanism may be of importance when identifying important sensory information in an environment with background activity, and may be an over-arching principal applicable to higher-order thalamic nuclei function in the control of cognitive and attentional processes. As the mGlu3 receptor subtype appears to be activated by endogenous 'glutamate spillover' upon afferent stimulation, it may be advantageous to develop mGlu3 PAMs, as opposed to direct agonists, to alleviate instances of increased thalamic inhibition, as is believed to occur in schizophrenia. Indeed, there is emerging evidence to suggest that mGlu3 PAMs could act to enhance performance in cognitive tasks (Walker and Conn, 2015).

Figure Legends

Figure 1. Thalamic circuitry underlying responses to vibrissal deflection. Branching collaterals from excitatory thalamocortical and corticothalamic axons (black), which originate from functionally linked topographical areas in the thalamus/cortex, innervate the TRN, and the TRN sends a reciprocal inhibitory projection (grey) back to the thalamic area from which it receives its thalamocortical innervation.

Figure 2. The Group II mGlu receptor agonist effect on evoked and spontaneous presynaptic quantal release events is nullified in mGlu3 knock-out mice. ai Traces of the effects of the Group II mGlu receptor agonist LY354740 (30nM) alone and in conjunction with increasing concentrations of the Group II mGlu receptor antagonist LY341495 (10nM, 30nM, 300nM) on IPSP amplitude in wild type mouse brain slices. **aii** Traces of the effects of the Group II mGlu receptor agonist LY354740 (30nM & 300nM) on IPSP amplitude in mGlu3 knock-out mouse brain slices. **bi** Overall effects on IPSP amplitude in wild type mouse brain slices of the same compound application combinations as described in **ai**. * indicates significance at the $p<0.05$ threshold of responses under drug conditions in comparison to baseline. **bii** Overall effects on IPSP amplitude in mGlu3 knock-out mouse brain slices of the same compound application combinations as described in **aii**. **ci** Traces from individual neurons illustrating the effects of the Group II mGlu receptor agonist LY354740 (30nM) alone or in conjunction with the Group II mGlu receptor antagonist LY341495 (100nM) on the number of spontaneous mIPSC events in the VB in wild type mouse brain slices. **cii** Traces from individual neurons illustrating the effects of the Group II mGlu receptor agonist LY354740 (30nM) on the number of spontaneous mIPSC events in the VB in mGlu3 knock-out mouse brain slices. **di** Effects of the same compound application combinations on the cumulative fraction of the calculated inter-event intervals of the spontaneous mIPSCs in the VB in wild type mouse brain slices as described in **ci**. **dii** Effects of the same compound application combinations on the cumulative fraction of the calculated inter-event intervals of the spontaneous mIPSCs in the VB in mGlu3 knock-out mouse brain slices as described in **cii**.

Figure 3. The mixed compound LY395756 (mGlu2 agonist, mGlu3 antagonist) reveals an mGlu3 component to the overall Group II mGlu receptor effect on sensory evoked inhibition. a Top: Timeline of a representative neuron response under baseline conditions (1), upon application of the mixed compound LY395756 alone (2), recovery (3), application of the mixed compound LY395756 together with the mGlu2 PAM LY487379 (4), and a second recovery (5). Bottom: PSTHs of responses of a VB neuron (CVB122c1) to train stimulation of a single vibrissa (40ms bins, 6 trials) under the conditions described in the above timeline. **b** Bars representing the % baseline response (±SEM) under baseline conditions (100%), in the presence of the mixed compound LY395756 alone, the mixed compound LY395756 in conjunction with the mGlu2 PAM LY487379, and during recovery. * indicates significance at the $p<0.05$ threshold of responses under drug conditions in comparison to baseline, unless otherwise indicated.

Figure 4. The mixed compound LY395756 when applied alone exerts effects similar to that of the Group II mGlu receptor antagonist LY341495. ai PSTHs delineating tonic (black) and burst (grey) responses of a VB neuron (CVB127b2) to train stimulation of a single vibrissa (50ms bins, 18 trials) under baseline conditions, upon application of the mixed compound LY395756, and during recovery. **aii** LHS: Bars representing the total % baseline response (±SEM) under the same conditions as described in **ai**. RHS: Bars representing the % of the response exhibited as burst firing (±SEM) under the same conditions as described in **ai**. **bi** PSTHs delineating tonic (black) and burst (grey) responses of a VB neuron (CVB087b1) to train stimulation of a single vibrissa (50ms bins, 18 trials) under baseline conditions, upon application of the Group II mGlu receptor antagonist LY341495, and during recovery. **bii** LHS: Bars representing the total % baseline response (±SEM) under the same conditions as

described in **bi**. RHS: Bars representing the % of the response exhibited as burst firing (±SEM) under the same conditions as described in **bi**. * indicates significance at the $p<0.05$ threshold of responses under drug conditions in comparison to baseline.

Figure 5. The mixed compound LY395756 when applied in conjunction with the mGlu2 PAM LY487379 exerts effects similar to that of the Group II mGlu receptor agonist LY354740. ai PSTHs delineating tonic (black) and burst (grey) responses of a VB neuron (CVB130a2) to train stimulation of a single vibrissa (50ms bins, 18 trials) under baseline conditions, upon application of the mixed compound LY395756 and the mGlu2 PAM LY487379, and during recovery. **aii** LHS: Bars representing the total % baseline response (±SEM) under the same conditions as described in **ai**. RHS: Bars representing the % of the response exhibited as burst firing (±SEM under the same conditions as described in **ai**. **bi** PSTHs delineating tonic (black) and burst (grey) responses of a VB neuron (CVB030a2) to train stimulation of a single vibrissa (50ms bins, 18 trials) under baseline conditions, upon application of the Group II mGlu receptor agonist LY354740, and during recovery. **bii** LHS: Bars representing the total % baseline response (±SEM) under the same conditions as described in **bi**. RHS: Bars representing the % of the response exhibited as burst firing (±SEM) under the same conditions as described in **bi**. * indicates significance at the $p<0.05$ threshold of responses under drug conditions in comparison to baseline.

Conflict of Interest

Authors: No conflicts to declare.

Declaration of transparency and scientific rigour: This Declaration acknowledges that this paper adheres to the principles for transparent reporting and scientific rigour of preclinical research as stated in the BJP guidelines for Design and Analysis, and Animal Experimentation, and as recommended by funding agencies, publishers and other organisations engaged with supporting research.

References

ALEXANDER, G. M. & GODWIN, D. W. 2005. Presynaptic inhibition of corticothalamic feedback by metabotropic glutamate receptors. *J Neurophysiol,* 94**,** 163-75.

ALEXANDER, G. M. & GODWIN, D. W. 2006. Unique presynaptic and postsynaptic roles of Group II metabotropic glutamate receptors in the modulation of thalamic network activity. *Neuroscience,* 141**,** 501-13.

Alexander SPH, Christopoulos A, Davenport AP, et al. THE CONCISE GUIDE TO PHARMACOLOGY 2019/20: G protein-coupled receptors. Br J Pharmacol. 2019;176(Suppl 1):S21–s141.

BARBARESI, P., SPREAFICO, R., FRASSONI, C. & RUSTIONI, A. 1986. GABAergic neurons are present in the dorsal column nuclei but not in the ventroposterior complex of rats. *Brain Res,* 382**,** 305-26.

BECKER, J. B., PRENDERGAST, B. J. & LIANG, J. W. 2016. Female rats are not more variable than male rats: a meta-analysis of neuroscience studies. *Biol Sex Differ,* 7**,** 34.

CEOLIN, L., KANTAMNENI, S., BARKER, G. R., HANNA, L., MURRAY, L., WARBURTON, E. C., ROBINSON, E. S., MONN, J. A., FITZJOHN, S. M., COLLINGRIDGE, G. L., BORTOLOTTO, Z. A. & LODGE, D. 2011. Study of novel selective mGlu2 agonist in the temporo-ammonic input to CA1 neurons reveals reduced mGlu2 receptor expression in a Wistar substrain with an anxiety-like phenotype. *J Neurosci,* 31**,** 6721-31.

CIEŚLIK, P., DOMIN, H., CHOCYK, A., GRUCA, P., LITWA, E., PŁOSKA, A., RADULSKA, A., PELIKANT-MAŁECKA, I., BRAŃSKI, P., KALINOWSKI, L. & WIEROŃSKA, J. M. 2020. Simultaneous activation of mGlu(2) and muscarinic receptors reverses MK-801-induced cognitive decline in rodents. *Neuropharmacology,* 174**,** 107866.

CONN, P. J. & PIN, J. P. 1997. Pharmacology and functions of metabotropic glutamate receptors. *Annu Rev Pharmacol Toxicol,* 37**,** 205-37.

COPELAND, C. S., NEALE, S. A. & SALT, T. E. 2012. Positive allosteric modulation reveals a specific role for mGlu2 receptors in sensory processing in the thalamus. *J Physiol,* 590**,** 937-51.

COPELAND, C. S., NEALE, S. A. & SALT, T. E. 2015. Neuronal activity patterns in the mediodorsal thalamus and related cognitive circuits are modulated by metabotropic glutamate receptors. *Neuropharmacology,* 92**,** 16-24.

COPELAND, C. S., WALL, T. M., SIMS, R. E., NEALE, S. A., NISENBAUM, E., PARRI, H. R. & SALT, T. E. 2017. Astrocytes modulate thalamic sensory processing via mGlu2 receptor activation. *Neuropharmacology,* 121**,** 100-110.

COX, C. L. & SHERMAN, S. M. 1999. Glutamate inhibits thalamic reticular neurons. *J Neurosci,* 19**,** 6694-9.

CURTIS, M. J., BOND, R. A., SPINA, D., AHLUWALIA, A., ALEXANDER, S. P., GIEMBYCZ, M. A., GILCHRIST, A., HOYER, D., INSEL, P. A., IZZO, A. A., LAWRENCE, A. J., MACEWAN, D. J., MOON, L. D., WONNACOTT, S., WESTON, A. H. & MCGRATH, J. C. 2015. Experimental design and analysis and their reporting: new guidance for publication in BJP. *Br J Pharmacol,* 172**,** 3461-71.

DENICOLA, A. L., PARK, M. Y., CROWE, D. A., MACDONALD, A. W., 3RD & CHAFEE, M. V. 2020. Differential Roles of Mediodorsal Nucleus of the Thalamus and Prefrontal Cortex in Decision-Making and State Representation in a Cognitive Control Task Measuring Deficits in Schizophrenia. *J Neurosci,* 40**,** 1650-1667.

DIAMOND, M. E., VON HEIMENDAHL, M., KNUTSEN, P. M., KLEINFELD, D. & AHISSAR, E. 2008. 'Where' and 'what' in the whisker sensorimotor system. *Nat Rev Neurosci,* 9**,** 601-12.

DOMINGUEZ, C., PRIETO, L., VALLI, M. J., MASSEY, S. M., BURES, M., WRIGHT, R. A., JOHNSON, B. G., ANDIS, S. L., KINGSTON, A., SCHOEPP, D. D. & MONN, J. A. 2005. Methyl substitution of 2-aminobicyclo[3.1.0]hexane 2,6-dicarboxylate (LY354740) determines functional activity at metabotropic glutamate receptors: identification of a subtype selective mGlu2 receptor agonist. *J Med Chem,* 48**,** 3605-12.

FERRARELLI, F. & TONONI, G. 2017. Reduced sleep spindle activity point to a TRN-MD thalamus-PFC circuit dysfunction in schizophrenia. *Schizophr Res,* 180**,** 36-43.

GALICI, R., ECHEMENDIA, N. G., RODRIGUEZ, A. L. & CONN, P. J. 2005. A selective allosteric potentiator of metabotropic glutamate (mGlu) 2 receptors has effects similar to an orthosteric mGlu2/3 receptor agonist in mouse models predictive of antipsychotic activity. *J Pharmacol Exp Ther,* 315**,** 1181-7.

HAIDARLIU, S., SIMONY, E., GOLOMB, D. & AHISSAR, E. 2010. Muscle architecture in the mystacial pad of the rat. *Anat Rec (Hoboken),* 293**,** 1192-206.

HANNA, L., CEOLIN, L., LUCAS, S., MONN, J., JOHNSON, B., COLLINGRIDGE, G., BORTOLOTTO, Z. & LODGE, D. 2013. Differentiating the roles of mGlu2 and mGlu3 receptors using LY541850, an mGlu2 agonist/mGlu3 antagonist. *Neuropharmacology,* 66**,** 114-21.

Harding, S.D., Sharman, J.L., Faccenda, E., Southan, C., Pawson AJ, Ireland S, Gray AJG, Bruce L, Alexander SPH, Anderton S, Bryant C, Davenport AP, Doerig C, Fabbro D, Levi-Schaffer F, Spedding M, Davies JA, NC-IUPHAR (2018). The IUPHAR/BPS Guide to PHARMACOLOGY in 2018: updates and expansion to encompass the new guide to IMMUNOPHARMACOLOGY. Nucleic Acids Res. 46, D1091-1106. doi:10.1093/nar/gkx1121.

HARRIS, R. M. & HENDRICKSON, A. E. 1987. Local circuit neurons in the rat ventrobasal thalamus--a GABA immunocytochemical study. *Neuroscience,* 21**,** 229-36.

JAHNSEN, H. & LLINÁS, R. 1984. Voltage-dependent burst-to-tonic switching of thalamic cell activity: an in vitro study. *Arch Ital Biol,* 122**,** 73-82.

JOHNSON, K. A., MATEO, Y. & LOVINGER, D. M. 2017. Metabotropic glutamate receptor 2 inhibits thalamically-driven glutamate and dopamine release in the dorsal striatum. *Neuropharmacology,* 117**,** 114-123.

JOHNSON, M. P., BAEZ, M., JAGDMANN, G. E., JR., BRITTON, T. C., LARGE, T. H., CALLAGARO, D. O., TIZZANO, J. P., MONN, J. A. & SCHOEPP, D. D. 2003. Discovery of allosteric potentiators for the metabotropic glutamate 2 receptor: synthesis and subtype selectivity of N-(4-(2-methoxyphenoxy)phenyl)-N-(2,2,2- trifluoroethylsulfonyl)pyrid-3-ylmethylamine. *J Med Chem,* 46**,** 3189-92.

JONES, E. G. 2009. Synchrony in the interconnected circuitry of the thalamus and cerebral cortex. *Ann N Y Acad Sci,* 1157**,** 10-23.

KINGSTON, A. E., ORNSTEIN, P. L., WRIGHT, R. A., JOHNSON, B. G., MAYNE, N. G., BURNETT, J. P., BELAGAJE, R., WU, S. & SCHOEPP, D. D. 1998. LY341495 is a nanomolar potent and selective antagonist of group II metabotropic glutamate receptors. *Neuropharmacology,* 37**,** 1-12.

KULLMANN, D. M. 2000. Spillover and synaptic cross talk mediated by glutamate and GABA in the mammalian brain. *Prog Brain Res,* 125**,** 339-51.

LINDEN, A. M., SHANNON, H., BAEZ, M., YU, J. L., KOESTER, A. & SCHOEPP, D. D. 2005. Anxiolytic-like activity of the mGLU2/3 receptor agonist LY354740 in the elevated plus maze test is disrupted in metabotropic glutamate receptor 2 and 3 knock-out mice. *Psychopharmacology (Berl),* 179**,** 284-91.

LIU, X. B., MUÑOZ, A. & JONES, E. G. 1998. Changes in subcellular localization of metabotropic glutamate receptor subtypes during postnatal development of mouse thalamus. *J Comp Neurol,* 395**,** 450-65.

LLINÁS, R. & JAHNSEN, H. 1982. Electrophysiology of mammalian thalamic neurones in vitro. *Nature,* 297**,** 406-8.

LOURENÇO NETO, F., SCHADRACK, J., BERTHELE, A., ZIEGLGÄNSBERGER, W., TÖLLE, T. R. & CASTRO-LOPES, J. M. 2000. Differential distribution of metabotropic glutamate receptor subtype mRNAs in the thalamus of the rat. *Brain Res,* 854**,** 93-105.

LU, S. M., GUIDO, W. & SHERMAN, S. M. 1992. Effects of membrane voltage on receptive field properties of lateral geniculate neurons in the cat: contributions of the low-threshold Ca2+ conductance. *J Neurophysiol,* 68**,** 2185-98.

LUCAS, S. J., BORTOLOTTO, Z. A., COLLINGRIDGE, G. L. & LODGE, D. 2013. Selective activation of either mGlu2 or mGlu3 receptors can induce LTD in the amygdala. *Neuropharmacology,* 66**,** 196-201.

MANGO, D., CARUSO, A., SAIDI, A., NISTICÒ, R. & SCACCIANOCE, S. 2019. The positive allosteric modulator at mGlu2 receptors, LY487379, reverses the effects of chronic stress-induced behavioral maladaptation and synaptic dysfunction in the adulthood. *Synapse,* 73**,** e22101.

MCGRATH, J. C., MCLACHLAN, E. M. & ZELLER, R. 2015. Transparency in Research involving Animals: The Basel Declaration and new principles for reporting research in BJP manuscripts. *Br J Pharmacol,* 172**,** 2427-32.

MINEFF, E. & VALTSCHANOFF, J. 1999. Metabotropic glutamate receptors 2 and 3 expressed by astrocytes in rat ventrobasal thalamus. *Neurosci Lett,* 270**,** 95-8.

MOLDRICH, R. X., CHAPMAN, A. G., DE SARRO, G. & MELDRUM, B. S. 2003. Glutamate metabotropic receptors as targets for drug therapy in epilepsy. *Eur J Pharmacol,* 476**,** 3-16.

MONN, J. A., VALLI, M. J., MASSEY, S. M., WRIGHT, R. A., SALHOFF, C. R., JOHNSON, B. G., HOWE, T., ALT, C. A., RHODES, G. A., ROBEY, R. L., GRIFFEY, K. R., TIZZANO, J. P., KALLMAN, M. J., HELTON, D. R. & SCHOEPP, D. D. 1997. Design, synthesis, and pharmacological characterization of (+)-2-aminobicyclo[3.1.0]hexane-2,6-dicarboxylic acid (LY354740): a potent, selective, and orally active group 2 metabotropic glutamate receptor agonist possessing anticonvulsant and anxiolytic properties. *J Med Chem,* 40**,** 528-37.

NORDQUIST, R. E., STECKLER, T., WETTSTEIN, J. G., MACKIE, C. & SPOOREN, W. 2008. Metabotropic glutamate receptor modulation, translational methods, and biomarkers: relationships with anxiety. *Psychopharmacology (Berl),* 199**,** 389-402.

OHARA, P. T. & LIEBERMAN, A. R. 1993. Some aspects of the synaptic circuitry underlying inhibition in the ventrobasal thalamus. *J Neurocytol,* 22**,** 815-25.

OHISHI, H., SHIGEMOTO, R., NAKANISHI, S. & MIZUNO, N. 1993a. Distribution of the messenger RNA for a metabotropic glutamate receptor, mGluR2, in the central nervous system of the rat. *Neuroscience,* 53**,** 1009-18.

OHISHI, H., SHIGEMOTO, R., NAKANISHI, S. & MIZUNO, N. 1993b. Distribution of the mRNA for a metabotropic glutamate receptor (mGluR3) in the rat brain: an in situ hybridization study. *J Comp Neurol,* 335**,** 252-66.

PARNAUDEAU, S., O'NEILL, P. K., BOLKAN, S. S., WARD, R. D., ABBAS, A. I., ROTH, B. L., BALSAM, P. D., GORDON, J. A. & KELLENDONK, C. 2013. Inhibition of mediodorsal thalamus disrupts thalamofrontal connectivity and cognition. *Neuron,* 77**,** 1151-62.

PAXINOS, G. & WATSON, C. 1986. *The rat brain in stereotaxic co-ordinates,* San Diego, CA, Academic Press.

PERÄKYLÄ, J., SUN, L., LEHTIMÄKI, K., PELTOLA, J., ÖHMAN, J., MÖTTÖNEN, T., OGAWA, K. H. & HARTIKAINEN, K. M. 2017. Causal Evidence from Humans for the Role of Mediodorsal Nucleus of the Thalamus in Working Memory. *J Cogn Neurosci,* 29**,** 2090-2102.

RALSTON, H. H. I. 1983. *The synaptic organization of the ventrobasal thalamus in the rat, cat and monkey. In Somatosensory Integration in the Thalamus.,* Amsterdam, Elsevier Science.

RAMCHARAN, E. J., GNADT, J. W. & SHERMAN, S. M. 2000. Burst and tonic firing in thalamic cells of unanesthetized, behaving monkeys. *Vis Neurosci,* 17**,** 55-62.

RIVADULLA, C., MARTINEZ, L., GRIEVE, K. L. & CUDEIRO, J. 2003. Receptive field structure of burst and tonic firing in feline lateral geniculate nucleus. *J Physiol,* 553**,** 601-10.

SALT, T. E. 1987. Excitatory amino acid receptors and synaptic transmission in the rat ventrobasal thalamus. *J Physiol,* 391**,** 499-510.

SALT, T. E. & EATON, S. A. 1995a. Distinct presynaptic metabotropic receptors for L-AP4 and CCG1 on GABAergic terminals: pharmacological evidence using novel alpha-methyl derivative mGluR antagonists, MAP4 and MCCG, in the rat thalamus in vivo. *Neuroscience,* 65**,** 5-13.

SALT, T. E. & EATON, S. A. 1995b. Modulation of sensory neurone excitatory and inhibitory responses in the ventrobasal thalamus by activation of metabotropic excitatory amino acid receptors. *Neuropharmacology,* 34**,** 1043-51.

712 SALT, T. E. & TURNER, J. P. 1998. Modulation of sensory inhibition in the ventrobasal thalamus via
713 activation of group II metabotropic glutamate receptors by 2R,4R-aminopyrrolidine-2,4-
714 dicarboxylate. *Exp Brain Res,* 121**,** 181-5.
715 SANGER, H., HANNA, L., COLVIN, E. M., GRUBISHA, O., URSU, D., HEINZ, B. A., FINDLAY, J. D., VIVIER,
716 R. G., SHER, E., LODGE, D., MONN, J. A. & BROAD, L. M. 2013. Pharmacological profiling of
717 native group II metabotropic glutamate receptors in primary cortical neuronal cultures using
718 a FLIPR. *Neuropharmacology,* 66**,** 264-73.
719 SCHOEPP, D. D., WRIGHT, R. A., LEVINE, L. R., GAYDOS, B. & POTTER, W. Z. 2003. LY354740, an mGlu2/3
720 receptor agonist as a novel approach to treat anxiety/stress. *Stress,* 6**,** 189-97.
721 SHERMAN, S. M. & GUILLERY, R. W. 2001. *Exploring the thalamus*, New York: Academic Press.
722 STANSLEY, B. J. & CONN, P. J. 2018. The therapeutic potential of metabotropic glutamate receptor
723 modulation for schizophrenia. *Curr Opin Pharmacol,* 38**,** 31-36.
724 STEULLET, P., CABUNGCAL, J. H., BUKHARI, S. A., ARDELT, M. I., PANTAZOPOULOS, H., HAMATI, F.,
725 SALT, T. E., CUENOD, M., DO, K. Q. & BERRETTA, S. 2018. The thalamic reticular nucleus in
726 schizophrenia and bipolar disorder: role of parvalbumin-expressing neuron networks and
727 oxidative stress. *Mol Psychiatry,* 23**,** 2057-2065.
728 TAMARU, Y., NOMURA, S., MIZUNO, N. & SHIGEMOTO, R. 2001. Distribution of metabotropic
729 glutamate receptor mGluR3 in the mouse CNS: differential location relative to pre- and
730 postsynaptic sites. *Neuroscience,* 106**,** 481-503.
731 TURNER, J. P. & SALT, T. E. 2003. Group II and III metabotropic glutamate receptors and the control of
732 the nucleus reticularis thalami input to rat thalamocortical neurones in vitro. *Neuroscience,*
733 122**,** 459-69.
734 WALKER, A. G. & CONN, P. J. 2015. Group I and group II metabotropic glutamate receptor allosteric
735 modulators as novel potential antipsychotics. *Curr Opin Pharmacol,* 20**,** 40-5.
736 YOUNG, A. & WIMMER, R. D. 2017. Implications for the thalamic reticular nucleus in impaired
737 attention and sleep in schizophrenia. *Schizophr Res,* 180**,** 44-47.

738

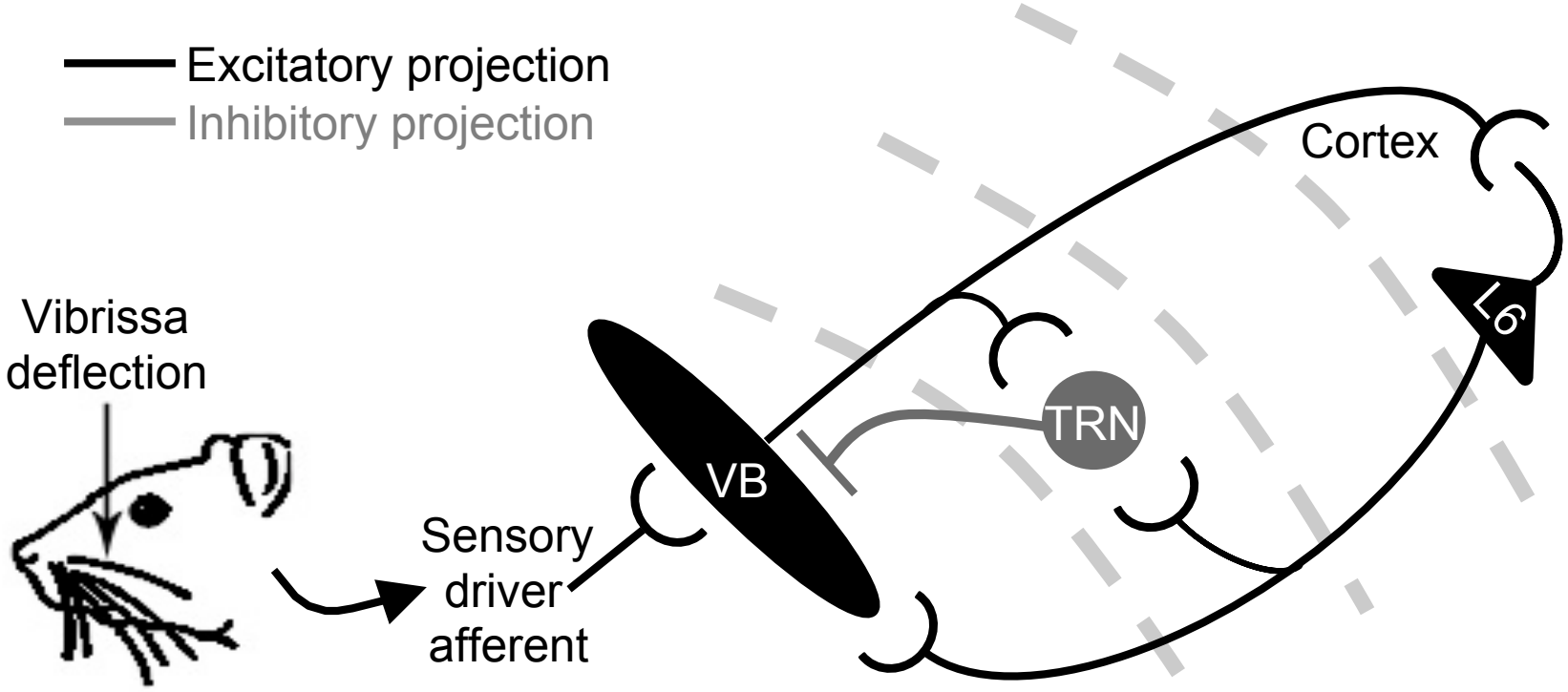
Excitatory projection
Inhibitory projection
Cortex
L6
TRN
VB
Vibrissa
deflection
Sensory
driver
afferent

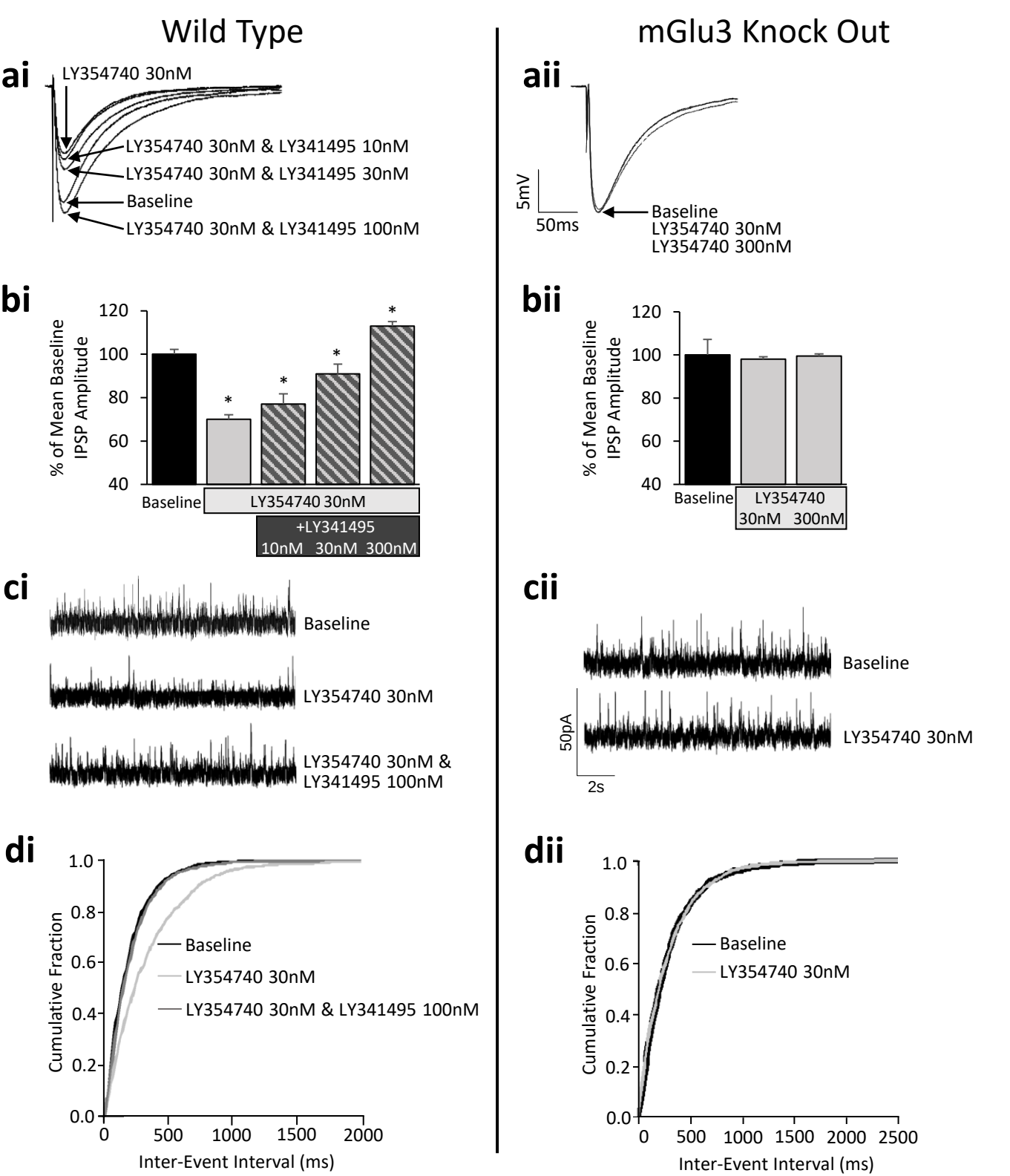
Wild Type
mGlu3 Knock Out
ai
LY354740 30nM
LY354740 30nM & LY341495 10nM
LY354740 30nM & LY341495 30nM
Baseline
LY354740 30nM & LY341495 100nM
aii
5mV
50ms
Baseline
LY354740 30nM
LY354740 300nM
bi
% of Mean Baseline IPSP Amplitude
120
100
80
60
40
*
Baseline
LY354740 30nM
+LY341495
10nM 30nM 300nM
bii
% of Mean Baseline IPSP Amplitude
120
100
80
60
40
Baseline
LY354740
30nM 300nM
ci
Baseline
LY354740 30nM
LY354740 30nM &
LY341495 100nM
cii
Baseline
50pA
2s
LY354740 30nM
di
Cumulative Fraction
1.0
0.8
0.6
0.4
0.2
0.0
0
500
1000
1500
2000
Inter-Event Interval (ms)
Baseline
LY354740 30nM
LY354740 30nM & LY341495 100nM
dii
Cumulative Fraction
1.0
0.8
0.6
0.4
0.2
0.0
0
500
1000
1500
2000
2500
Inter-Event Interval (ms)
Baseline
LY354740 30nM

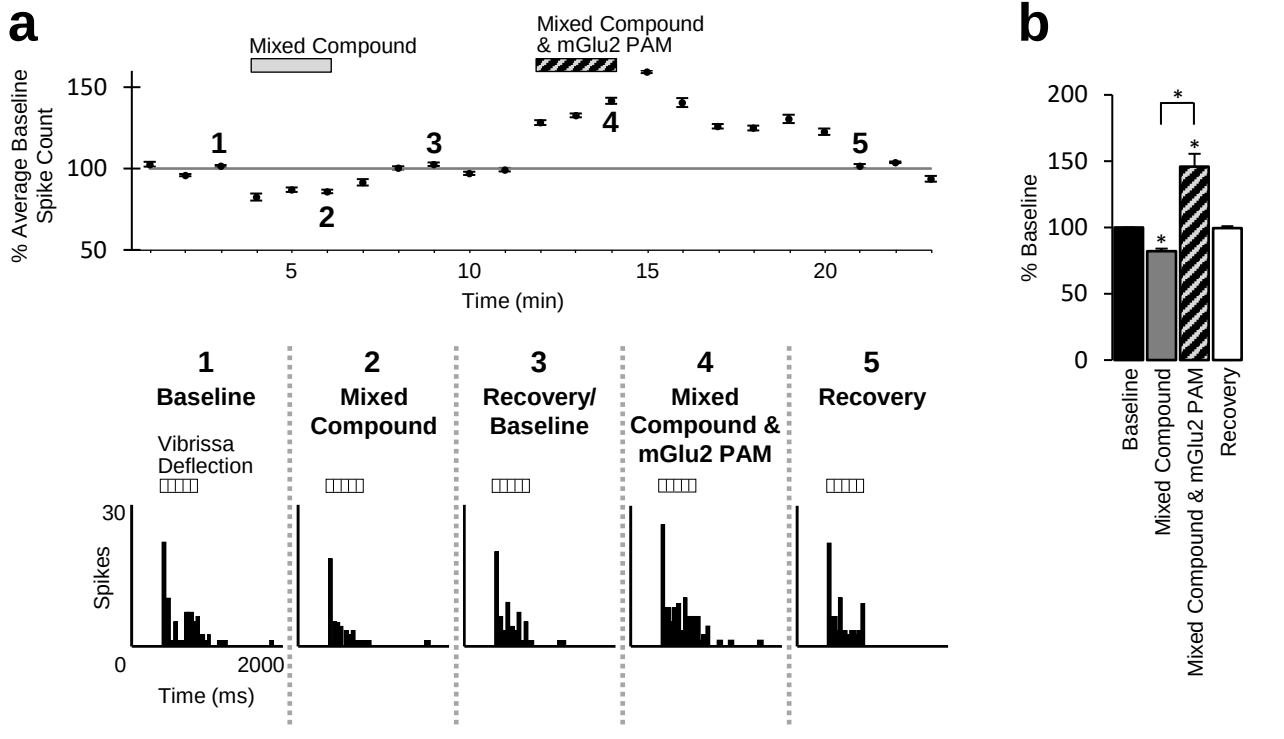
a
Mixed Compound
Mixed Compound
& mGlu2 PAM
% Average Baseline
Spike Count
150
100
50
1
2
3
4
5
5
10
15
20
Time (min)
1
Baseline
2
Mixed
Compound
3
Recovery/
Baseline
4
Mixed
Compound &
mGlu2 PAM
5
Recovery
Vibrissa
Deflection
30
Spikes
0
2000
Time (ms)
b
200
150
100
50
0
% Baseline
*
*
*
Baseline
Mixed Compound
Mixed Compound & mGlu2 PAM
Recovery

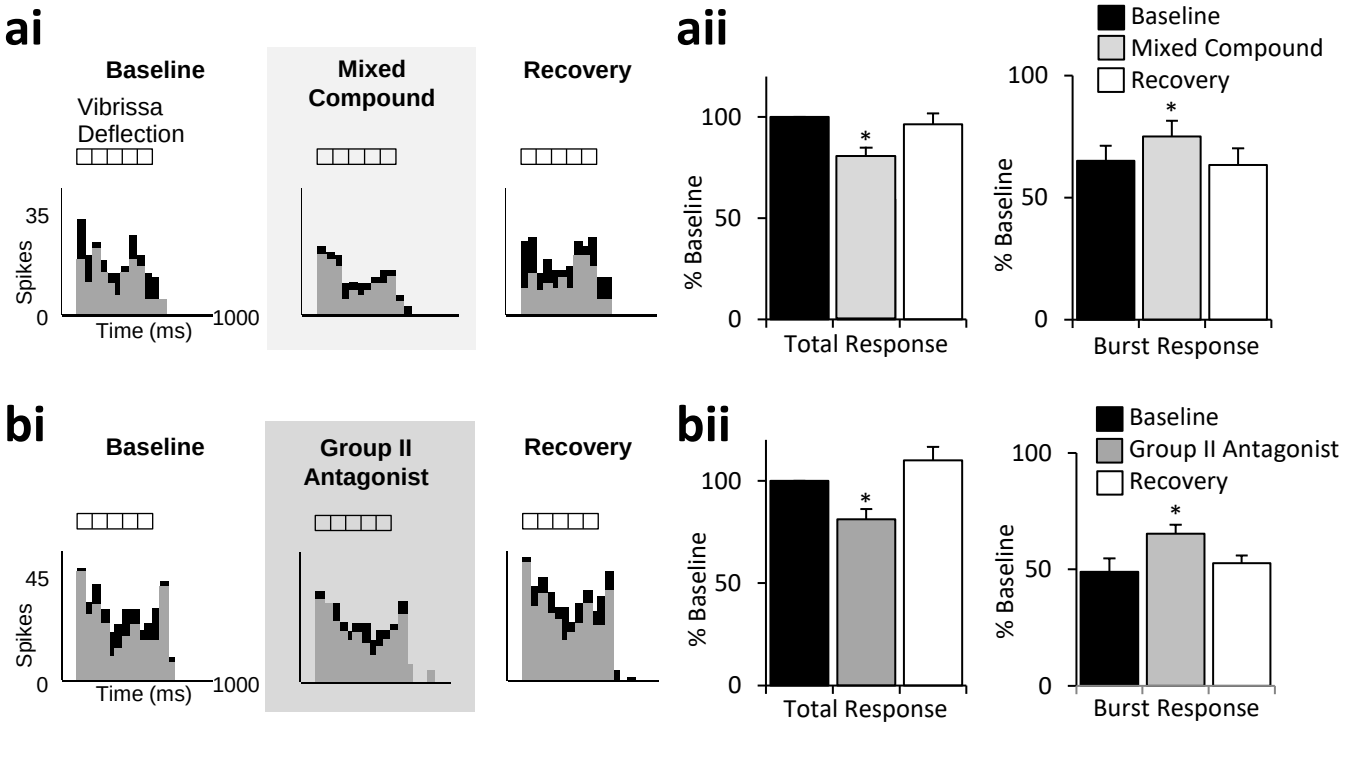
ai
Baseline
Mixed Compound
Recovery
Vibrissa Deflection
35
Spikes
0
Time (ms)
1000
aii
Baseline
Mixed Compound
Recovery
100
50
0
% Baseline
*
Total Response
Burst Response
bi
Baseline
Group II Antagonist
Recovery
45
bii
Group II Antagonist

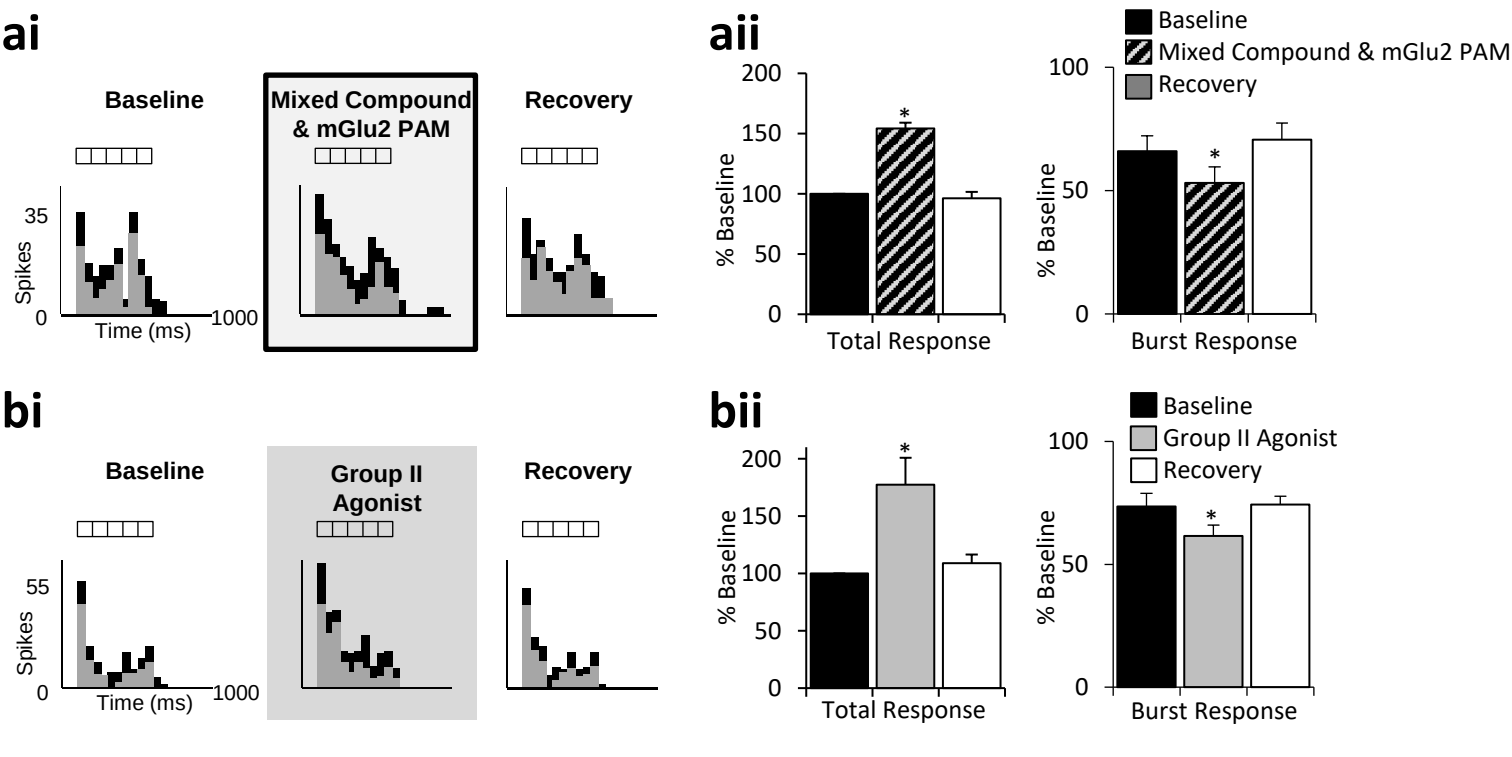
ai
Baseline
Mixed Compound & mGlu2 PAM
Recovery
35
Spikes
0
Time (ms)
1000
aii
Baseline
Mixed Compound & mGlu2 PAM
Recovery
200
150
100
50
0
% Baseline
*
Total Response
100
50
0
% Baseline
*
Burst Response
bi
Baseline
Group II Agonist
Recovery
55
Spikes
0
Time (ms)
1000
bii
Baseline
Group II Agonist
Recovery
200
150
100
50
0
% Baseline
*
Total Response
100
50
0
% Baseline
*
Burst Response